Solid-State Electronics 109 (2015) 12–16

Contents lists available at ScienceDirect

Solid-State Electronics

journal homepage: www.elsevier.com/locate/sse

Analysis of different forward current–voltage behaviours of Al implanted 4H-SiC vertical p–i–n diodes

M.L. Megherbi [a], F. Pezzimenti [b], L. Dehimi [a,c], S. Rao [b,*], F.G. Della Corte [b]

[a] Laboratory of Metallic and Semiconducting Materials, Mohammed Kheider University, 07000 Biskra, Algeria
[b] DIIES – Università Mediterranea di Reggio Calabria, Via Graziella, 89122 Reggio Calabria, Italy
[c] Faculty of Science, Elhadj Lakhdar University, 05000 Batna, Algeria

ARTICLE INFO

Article history:
Received 27 September 2014
Received in revised form 18 February 2015
Accepted 2 March 2015
Available online 22 March 2015

Keywords:
p–i–n diode
Silicon carbide
Device simulation
Carrier lifetime

ABSTRACT

In this work different experimental current–voltage behaviours of several Al implanted 4H-SiC p–i–n diodes are investigated by means of numerical simulations in a wide range of currents and temperatures. Some devices for which recombination and tunneling are the dominant current processes at all biases are classified as "leaky" diodes. The well behaved diodes, instead, show good rectifying characteristics with a current conduction due to tunneling below 1.7 V, recombination between 1.7 V and 2.5 V, and diffusion processes above 2.5 V. At higher current regimes, a series resistance in excess of 1 mΩ cm^2 becomes the main current limiting factor. Depending on the relative weight between the contact resistances and the internal diode resistance, different temperature dependencies of the current are obtained. A good agreement between numerical and measured data is achieved employing temperature-dependent carrier lifetime and mobility as fitting parameters.

1. Introduction

Silicon carbide (SiC) is a wide band-gap semiconductor with interesting physical properties in order to realize electronic devices well suited to operate under high-temperature, high-power, and/or high-radiation conditions. The potentials of the 4H-SiC polytype, in particular, are expected to enable significant improvements to a far ranging variety of applications and systems [1–5]. However, since this is a relatively new technology, intensive efforts are still necessary to ascertain the detailed physics and the real design benefits that can be obtained by developing simple SiC-based devices. To this extent, in this paper different forward *J–V* behaviours of several Al implanted 4H-SiC vertical p–i–n diodes are investigated by means of measurements and numerical simulations in a wide range of currents and temperatures. In details, diode experimental data and results of a proprietary simulation software [6] are combined to extract key physical parameters, including temperature dependent carrier lifetime and mobility, which aid to differentiate the current transport mechanisms at different biases. The current–voltage characteristics of well behaved and leaky diodes, realised with the some fabrication process, are presented. In addition, the role of the diode internal resistance in determining a crossing point from a positive to a negative temperature coefficient of the current [7–9] is reconsidered by simulations.

The realization of 4H-SiC p–i–n diodes with a negative temperature coefficient of the forward current could be well suitable for stable applications using parallel devices. This study could also turn useful in the design of more complex 4H-SiC power devices, such as the various JFET-based devices recently presented in literature [10–13], where p–i–n diodes are the embedded structures determining the device on- and off-state characteristics.

2. Device structure

The schematic cross-section (plot not in scale) of the investigated Al implanted p–i–n diodes and the calculated net doping profile along the vertical axis of symmetry of a device realized using a 5 μm-thick and 3×10^{15} cm^{-3}-doped epilayer, are shown in Fig. 1.

The diodes were provided by the CNR Institute for Microelectronics and Microsystems – Unit of Bologna (Italy). Details about the adopted technology were provided in [7] and references therein. In short, starting from a commercially available $\langle 0001 \rangle$ 8° off-axis 4H-SiC n-type homoepitaxial wafer of elevated crystal quality [14], the diode structure consists of a n$^+$ substrate with a doping concentration in the order of 10^{19} cm^{-3}, a 3×10^{15} cm^{-3} n$^-$ epilayer and a p$^+$ anode region obtained by

* Corresponding author.
E-mail address: sandro.rao@unirc.it (S. Rao).

http://dx.doi.org/10.1016/j.sse.2015.03.001

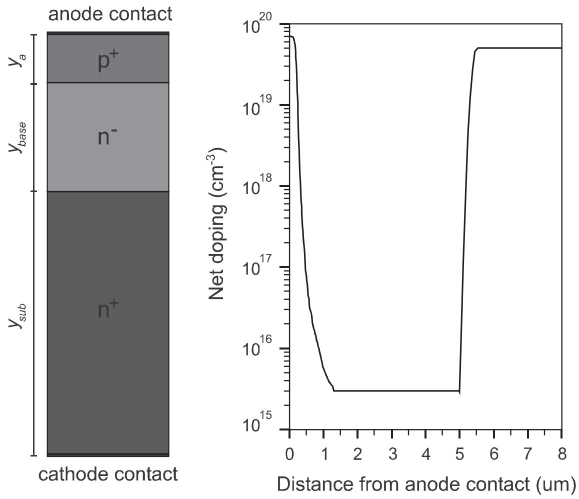

Fig. 1. 4H-SiC p–i–n diode schematic cross-section and net doping profile of a device with a 3×10^{15} cm^{-3}-doped epilayer.

aluminium implant. For the device in Fig. 1 (structure #1) the anode region exhibits a smooth half-Gaussian shaped profile with a peak doping of 6×10^{19} cm^{-3} at the surface, a profile edge located at about 0.2 µm and a profile tail crossing the epilayer doping at 1.35 µm, as verified by SIMS measurements. Almost similar diodes (structure #2) realized using a wafer with an epilayer thickness of 16.5 µm have also been analysed in this paper. The device ohmic contacts are made of a deposited Ni film on the back, while Ti/Al dots were deposited on the anode surface. Details about the implantation process and the post–implantation annealing are again reported in [7]. There, in particular, mainly depending on different post-implantation thermal treatments of the samples, two different anode contact resistances in the order of 1.25×10^{-3} Ω cm^2 and 2×10^{-5} Ω cm^2 were measured at room temperature for the structures labelled #1 and #2 in Table 1, respectively. For all the samples, the calculated active area is in the range 0.75–1 $\times 10^{-3}$ cm^2.

3. Physical models

The simulation analysis was carried out using the Silvaco's ATLAS simulator. The fundamental 4H-SiC physical models taken into account, such as the incomplete ionization of dopants, the band-gap temperature dependence, the carrier mobility and the carrier lifetime as a function both of doping and temperature, are briefly recalled as follows.

3.1. Incomplete ionization

Due to the wide bandgap of SiC, not all doping atoms can be assumed as fully activated. Using the Fermi–Dirac statistics, the carrier concentration N_a^- and N_d^+ (i.e. the number of ionized acceptors and donors) can be calculated with the expression [15]:

$$N_{a}^{-},{}_{d}^{+} = N_{a,d}\left(\frac{-1+\sqrt{1+4g_{a,d}\frac{N_{a,d}}{N_{V,C}(T)}e^{\frac{\Delta E_{a,d}}{kT}}}}{2g_{a,d}\frac{N_{a,d}}{N_{V,C}(T)}e^{\frac{\Delta E_{a,d}}{kT}}}\right) \quad (1)$$

where, N_V and N_C are the hole and electron density of states varying with temperature, N_a and N_d are the p-type and n-type doping concentrations, ΔE_a and ΔE_d are the acceptor and donor energy levels, and $g_a = 4$ and $g_d = 2$ are the appropriate degeneracy factors of the valence and conduction band. Considering the nature of the doping species (i.e. Al and N), an ionization energy level ΔE_a = 190 meV and ΔE_d = 70 meV is assumed [16,17].

3.2. Band gap model

The temperature dependence of the 4H-SiC band-gap is [18]:

$$E_g(T) = E_{g0} - \frac{\alpha T^2}{\beta + T} \quad (2)$$

where E_{g0} = 3.26 eV is the assumed band-gap energy at 300 K, $\alpha = 3.3 \times 10^{-4}$ eV/K and $\beta = 0$ are specific material parameters and T is the lattice temperature.

An apparent band-gap narrowing effect as a function of the activated doping in the p-type and n-type regions, i.e. ΔE_{ga} and ΔE_{gd} respectively, is also included during the simulations according to the Lindefelt's model of the band edge displacements [19]:

$$\Delta E_{ga} = A_a\left(\frac{N_a^-}{10^{18}}\right)^{1/2} + B_a\left(\frac{N_a^-}{10^{18}}\right)^{1/3} + C_a\left(\frac{N_a^-}{10^{18}}\right)^{1/4} \quad (3a)$$

$$\Delta E_{gd} = A_d\left(\frac{N_d^+}{10^{18}}\right)^{1/2} + B_d\left(\frac{N_d^+}{10^{18}}\right)^{1/3} + C_d\left(\frac{N_d^+}{10^{18}}\right)^{1/4} \quad (3b)$$

where $A_{a,d}$, $B_{a,d}$ and $C_{a,d}$, are appropriate 4H-SiC constants.

3.3. Mobility models

The low electric field mobility is modelled by the Caughey–Thomas empirical equation validated for 4H-SiC in [20]:

$$\mu_{n,p} = \mu_{0n,p}^{min}\left(\frac{T}{300}\right)^{\alpha_{n,p}} + \frac{\mu_{0n,p}^{max}\left(\frac{T}{300}\right)^{\beta_{n,p}} - \mu_{0n,p}^{min}\left(\frac{T}{300}\right)^{\alpha_{n,p}}}{1+\left(\frac{T}{300}\right)^{\gamma_{n,p}}\left(\frac{N}{N_{n,p}^{crit}}\right)^{\delta_{n,p}}} \quad (4)$$

where N is the local (total) concentration of the ionized impurities. The model parameters μ_0^{min}, μ_0^{max}, N^{crit}, α, β, δ, and γ, are taken from [18,20] and summarized in Table 2.

For high electric fields a carrier mobility reduction due to a carrier saturated drift velocity of 2×10^7 cm/s is considered as described in [10].

3.4. Carrier lifetimes

The carrier lifetimes useful to define the Shockley–Read–Hall recombination rate are modelled as functions of doping and

Table 1
Geometrical and doping parameters of different 4H-SiC p–i–n diodes.

	Structure #1 (D1)	Structure #2 (D2)
Anode thickness, Y_a (µm)	0.2	0.5
Anode doping (cm^{-3})	6×10^{19}	1×10^{20}
Base thickness, Y_{base} (µm)	4.8	16
Base doping (cm^{-3})	3×10^{15}	3×10^{15}
Cathode thickness, Y_{sub} (µm)	300	350
Cathode doping (cm^{-3})	5×10^{19}	1×10^{19}

Table 2
4H-SiC carrier mobility parameters.

	n	p
μ_0^{min} (cm^2/V s)	40	15.9
μ_0^{max} (cm^2/V s)	950	125
N^{crit} (cm^{-3})	2×10^{17}	1.76×10^{19}
α	−0.5	−0.5
β	−2.4	−2.15
δ	0.76	0.34
γ	−0.76	−0.34